

A zonogon approach for computing small polygons of maximum perimeter

Bernd Mulansky^{1†} and Andreas Potschka^{1*†}

^{1*}Institute of Mathematics, Clausthal University of Technology,
Erzstr. 1, 38678 Clausthal-Zellerfeld, Germany.

*Corresponding author(s). E-mail(s): andreas.potschka@tu-clausthal.de;
Contributing authors: bernd.mulansky@tu-clausthal.de;

[†]These authors contributed equally to this work.

Abstract

We derive a mixed integer nonlinear programming formulation for the problem of finding a convex polygon with a given number of vertices that is small (diameter at most one) and has maximum perimeter. The formulation is based on a geometric construction using zonogons. The resulting zonogons can be characterized by an integer code and we study the number of codes that are distinct under the symmetries of the problem. We propose a two-phase computational approach. Phase I comprises the solution of a purely combinatorial problem. Under assumption of Mossinghoff's conjecture, the Phase I problem can be reduced to a Subset-Sum Problem. Without Mossinghoff's conjecture, a generalized Subset-Sum Problem needs to be solved, which consists of picking n non-opposing $2n$ -th roots of unity such that their sum is as small as possible. Phase II consists of a non-combinatorial Nonlinear Programming Problem, which can be solved to high accuracy with arbitrary precision Newton-type methods. We provide extensive numerical results including highly accurate solutions for polygons with 64 and 128 vertices.

Keywords: Isodiametric problem, convex polygon, maximum perimeter, sums of roots of unity

MSC Classification: 52-08 , 52-A10 , 52-A38

1 Introduction

Let SP_n denote the set of convex polygons in the plane with $n \geq 3$ vertices that have diameter at most one. Its elements are called *small n -gons*. More than one hundred years ago, Reinhardt [1] asked which polygons in SP_n have maximum area or maximum perimeter. Reinhardt gave an answer to the area problem for odd n (the regular n -gon) and for the perimeter problem for all n with an odd divisor (via a construction with Reuleaux polygons). But even after a century of efforts by various bright minds, the perimeter problem is still open for the case when n is a power of two.

We follow here an experimental mathematics approach, hoping that numerical solutions of a number of medium range n might reveal the patterns that will eventually lead to a proof for settling Reinhardt's problems completely. From a numerical optimization point of view, the area problem is considered an important benchmark problem, which is listed in the COPS suite [2]. The computational results in [3] for hexagons and in [4] for octagons, for instance, justified the conjecture that the small polygons of maximum area with an even number n of vertices have a cycle of $n - 1$ diameter chords with one pending diameter chord attached. This conjecture was eventually proved in [5].

Such a result is missing for the perimeter problem, which motivates us to study novel computational methods to solve the perimeter problem for moderate sizes of n .

The small hexagon of largest area is well-known since its appearance in [3], or, perhaps, even since [6]. The value of its area turns out to be an algebraic number, namely a root of a polynomial of degree ten with integer coefficients. The small octagon of largest area was determined in [4]. As established later in [7], the maximum area of a small octagon is a root of an integer polynomial of degree 42.

These results suggest asking for similar representations of the longest perimeters. The longest perimeter of a small octagon was computed in [4], but it was already stated to four correct digits in [8]. The representation as an algebraic number was still missing. We show that the square of the longest perimeter of a small octagon is a root of an integer polynomial of degree 48.

For the perimeter $p(P_n)$ of a polygon $P_n \in SP_n$, Reinhardt [1] derived the upper bound

$$p(P_n) \leq 2n \sin \frac{\pi}{2n} =: \bar{u}_n < \pi.$$

For the case of n having an odd divisor $d \geq 3$, he proposed a construction based on Reuleaux d -gons to show that this upper bound can be attained by polygons with a rotational d -symmetry. Additional global maxima were discovered in [10] and baptized "sporadic". Ironically, it turned out that these non-Reinhardtian solutions are actually more frequent than Reinhardt's for larger n [11].

The missing cases $n = 2^s$, $s \geq 2$, have so far only been solved for $n = 4$ [12, 13] and $n = 8$ [14].

Mossinghoff's entertaining article in the American Mathematical Monthly [15] in 2006, together with his paper [16] helped to spark interest in the perimeter problem again. Before 2006, the interest in the problem has been rather infrequent, with a few notable contributions [12, 17, 18]. Fejes Tóth has recently added a chapter on the topic to the classic [19].

A currently highly active line of research is to improve asymptotic lower bounds for the gap between $p(P_n^*)$ and \bar{u}_n for novel constructions of $P_n^* \in \text{SP}_n$ (see, e.g., [16, 20–22]), which have been improved to

$$\bar{u}_n - p(P_n^*) \leq \frac{\pi^9}{8n^8} + O(n^{-10}). \quad (1)$$

We shall see in the second column of Tab. 3 that this bound overestimates the optimal gap considerably for $n = 32, 64, 128$.

1.1 Contributions

The paper at hand will also not give a complete solution of the perimeter problem. Instead, we present a Mixed-Integer Nonlinear Programming Problem (MINLP) that is equivalent to the perimeter problem under the conjecture that optimal polygons have n distinct diameters. We count the number of *codes* (the integer part of the solutions) that are distinct under dihedral symmetry (see Tab. 1). For a fixed code, the MINLP reduces to a continuous Nonlinear Programming Problem (NLP) with $n - 1$ variables, two equality constraints and n inequality constraints. We were not able to discover multiple local extrema for a fixed code NLP numerically, but we are not able to provide a proof for uniqueness of the NLP solution. For $n = 8$, we display the local maxima for each of the eleven distinct codes in Fig. 1 along with their perimeters in Tab. 2. We also enumerated all codes for the cases $n = 16$ and $n = 32$ and computed local maxima for each code. Fig. 2 shows the three local solutions for $n = 32$ with the largest perimeters, which coincide in the first thirteen decimal places. Hence, high-precision arithmetic is required for reliably computing solutions for larger n .

We further propose a two-phase algorithm to compute excellent suboptimal solutions of the MINLP by solving first a linear combinatorial Subset-Sum Problem (SSP) to generate codes and, second, solving a continuous nonlinear problem with fixed code using Newton-type methods with arbitrary precision arithmetic. The derivation of the SSP exploits Mossinghoff’s conjecture [16], which says that optimal small n -gons are axially symmetric. The resulting solutions for $n \leq 32$ coincide with the best local maxima in the full enumeration approach, and we confirm the current record of [22], but are able to compute the perimeter to arbitrary precision for the first time. We also provide a candidate polygon with large perimeter, which is as close as $2 \cdot 10^{-38}$ to the upper bound \bar{u}_{128} . Such computations were not possible with the computational methods available before. The resulting polygons are depicted in Fig. 3 along with the distance of their respective perimeters to the upper bound \bar{u}_n in Tab. 3.

Moreover, we show that the maximum perimeter of the small octagon is an algebraic number.

1.2 Structure

In Sec. (2), we use a zonogon construction to derive a MINLP for the perimeter problem. We discuss the combinatorics of the problem in Sec. 3 and propose a two-phase algorithm to compute polygons with large perimeter to arbitrary accuracy in Sec. 4. We present our computational experience with the two-phase approach in

n	#Codes
4	1
8	11
16	1,087
32	$33,570,815 \approx 3.4 \cdot 10^7$
64	$72,057,595,111,669,759 \approx 7.2 \cdot 10^{16}$
128	$664,613,997,892,457,941,063,589,548,567,560,191 \approx 6.6 \cdot 10^{35}$

Table 1: The number of distinct codes for the MINLPs (6) and (7) for $n = 2^s$.

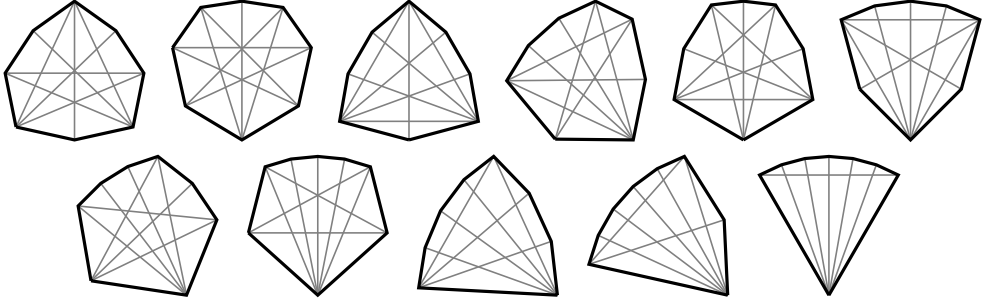


Fig. 1: Eleven small octagons with locally maximal perimeter, ordered with decreasing perimeter from left to right and top to bottom. The diameter graph, also known as the skeleton of the polygon, is depicted in gray.

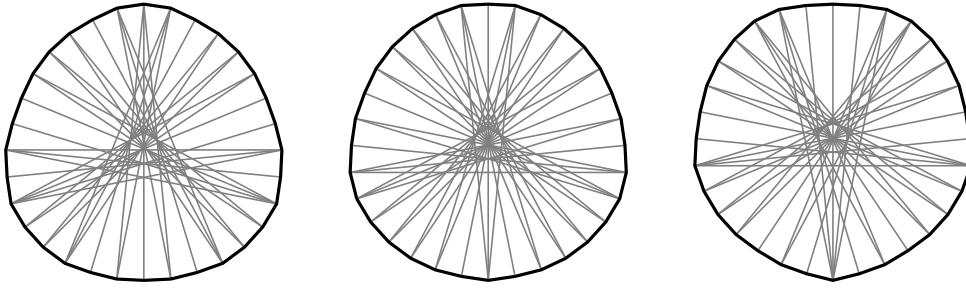
Rank	Perimeter	
1		3.121147134059831353864659503638086530909542. . .
2		3.119597665200247590150972423994095000480919. . .
3	$12 \sin \frac{\pi}{18} + 4 \sin \frac{\pi}{12}$	3.119054312413247235616194871727970865400783. . .
4		3.116482146091382523455235401221637774453205. . .
5		3.114973336127984895463908314651370982428416. . .
6	$8 \sin \frac{\pi}{24} + 8 \sin \frac{\pi}{12}$	3.114761898580578831178440524156298708342476. . .
7		3.108103162518355196717979437084906769281062. . .
8		3.103535201958031713403480443438109805364658. . .
9	$1 + 6 \sin \frac{\pi}{18} + 8 \sin \frac{\pi}{24}$	3.086098603761994825497549583779800857552179. . .
10	$1 + 4 \sin \frac{\pi}{12} + 10 \sin \frac{\pi}{30}$	3.080560813086617763393936898521174504202834. . .
11	$2 + 12 \sin \frac{\pi}{36}$	3.045868912971898082696771250049682616532413. . .

Table 2: Perimeters of the small polygons in Fig. 1 with exact formulas for the cases where the octagon can be constructed from an equilateral triangle.

Sec. 5. Finally, we show that the maximum perimeter for the octagon is an algebraic number in Sec. 6 and provide the corresponding integer polygon in the Appendix.

2 MINLP derivation using zonogons

Let P be a planar convex polygon with $n \geq 3$ vertices $v_1, \dots, v_n \in \mathbb{C}$, enumerated in counterclockwise order. We interpret P here as a closed subset of \mathbb{C} in the sense of the



3.140331156954619...

3.140331156954543...

3.140331156954350...

Fig. 2: Three small triacontadigons (32-gons) with locally maximal perimeter. The first 13 decimal digits of the perimeter (underlined) coincide.

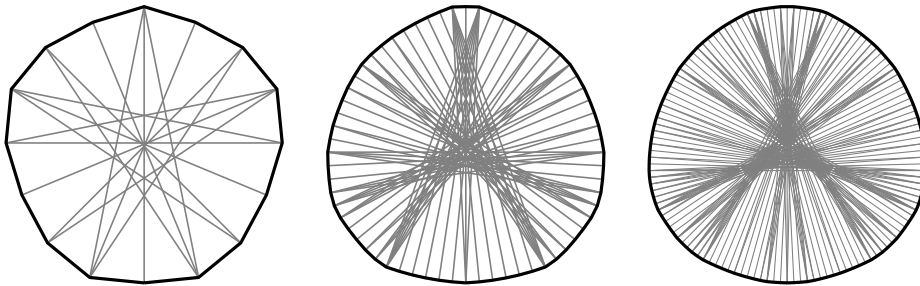


Fig. 3: Current perimeter records of small n -gons for $n = 2^s$, $s = 4, 6, 7$ (with $s = 5$ being depicted in Fig. 2, left).

n	$\pi^9/(8n^8)$	$\bar{u}_n - p(P_n)$	Perimeter $p(P_n)$
4	$5.686 \cdot 10^{-2}$	$2.619 \cdot 10^{-2}$	3.03527618041008304939559535049619331339627560527972205 ↔ 52560128292602278989952079876894718987769986620...
8	$2.221 \cdot 10^{-4}$	$2.980 \cdot 10^{-4}$	3.12114713405983135386465950363808653090954216646976012 ↔ 24524789123816403490428894959252350355455226792...
16	$8.676 \cdot 10^{-7}$	$7.741 \cdot 10^{-7}$	3.13654771648660738608596703194122822729813676580923269 ↔ 27892182035777457554738176289058573625428211593...
32	$3.389 \cdot 10^{-9}$	$1.335 \cdot 10^{-13}$	3.14033115695461936582540138057745867231205309833952186 ↔ 99104148559468837774634543964164383698560055119...
64	$1.324 \cdot 10^{-11}$	$2.836 \cdot 10^{-23}$	3.14127725093277286806199141550246829795626209630809641 ↔ 11750773439718362183509788657317267672710085186...
128	$5.171 \cdot 10^{-14}$	$1.816 \cdot 10^{-38}$	3.14151380114430107632851505945682230791714977539831260 ↔ 12200604676901080305902623648703203853047686174...

Table 3: Perimeters of the polygons of Fig. 3, their distances to Reinhardt's upper bound, and the asymptotic $\pi^9/(8n^8)$. The known solution $2 + 4 \sin \frac{\pi}{12}$ for $n = 4$ is provided for comparison.

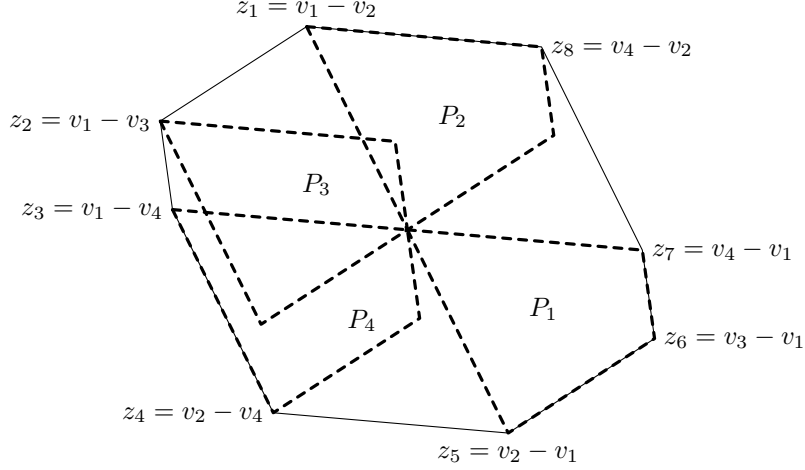


Fig. 4: Construction of the zonogon Z (solid edges) from the shifts P_1, P_2, P_3, P_4 (dashed edges) of the polygon P .

convex hull of its vertices $P = \text{co}\{v_1, \dots, v_n\}$. Let us consider n shifts of P defined by

$$P_l = P - v_l, \quad l = 1, \dots, n,$$

i.e., the l -th vertex of P is moved to the origin. The convex hull (compare Fig. 4)

$$Z = \left\{ \sum_{k,l=1}^n \lambda_{kl}(v_k - v_l) \mid \sum_{k,l=1}^n \lambda_{kl} = 1, \lambda_{kl} \geq 0, k, l = 1, \dots, n \right\} \quad (2)$$

of the shifted polygons P_1, \dots, P_n is the *zonogon* generated by P . Indeed, if $z \in Z$, then $-z \in Z$ by transposition of λ , which means that Z is centrally symmetric with respect to the origin.

Lemma 1. *The zonogon Z is contained in the unit disc if and only if P is small.*

Proof. Let $|z| \leq 1$ for all $z \in Z$. Choosing $\lambda_{kl} = 1$ (and all other components zero) delivers $v_k - v_l \in Z$, hence $|v_k - v_l| \leq 1$ for all $k, l = 1, \dots, n$. Hence, P is small.

Now assume $|v_k - v_l| \leq 1$ for all $k, l = 1, \dots, n$. Then, $|z| = \left| \sum_{k,l=1}^n \lambda_{kl}(v_k - v_l) \right| \leq \sum_{k,l=1}^n \lambda_{kl} = 1$. \square

Because P is a convex polygon, the zonogon Z is polygonal as well. By the representation (2) of Z as convex hull of the points $v_k - v_l$, its vertices have to be of this form. Choosing a vertex of Z as a start, we traverse the vertices counterclockwise to get

$$z_j = v_{k_j} - v_{l_j}, \quad k_j, l_j \in \{1, \dots, n\}, \quad j = 1, \dots, 2n.$$

The index tuples (k_j) and (l_j) are such that for each j either

$$k_{j+1} = k_j + 1 \quad \text{and} \quad l_{j+1} = l_j, \quad (3)$$

which means a move along the side $v_{k_j}v_{k_{j+1}}$ of P_{l_j} , or

$$k_{j+1} = k_j \quad \text{and} \quad l_{j+1} = l_j + 1, \quad (4)$$

which means a move to the vertex v_{k_j} of the next shift $P_{l_{j+1}}$.¹ After visiting all vertices of Z we return to z_1 . Then the indices k_j and l_j have been incremented n times each, which yields that Z has $2n$ vertices. We will assume that P does not have parallel sides, which implies that the vertices of Z are nondegenerate.

Definition 1. *Let P be a convex polygon such that the generated zonogon Z has $2n$ vertices. We define the code of P as $c = (c_1, \dots, c_{2n}) \in \{\pm 1\}^{2n}$, where $c_j := 1$ if (3) holds respectively $c_j := -1$ if (4) holds.*

The dependence of the code on the choice of the start vertex is not problematic, because we always consider equivalence classes of codes, where two codes c and c' are equivalent if there is an element of the dihedral group $\sigma \in D_{2n}$ such that $c_{\sigma(j)} = c'_j$ for $j = 1, \dots, 2n$, see section 3. It is most convenient to assign the signs c_j to the sides $z_{j+1} - z_j$ of Z . We remark that $c_{n+j} = -c_j$ for $j = 1, \dots, n$, because exactly one of the two opposite sides of Z is a side of one of the shifts of P . The code corresponding to Fig. 4 is $c = (- - + - + + - +)$, where the signs in the shortened notation have to be expanded to ± 1 . The corresponding index tuples are

$$k = (1, 1, 1, 2, 2, 3, 4, 4) \quad \text{and} \quad l = (2, 3, 4, 4, 1, 1, 1, 2).$$

Note that k and l , considered as circular tuples, are just rotations of each other.

We now parametrize the vertices of Z in polar form as

$$z_j = d_j \exp(i\varphi_j) \quad \text{for } j = 1, \dots, 2n.$$

The central symmetry of Z dictates that $z_{n+j} = -z_j$, i.e. $d_{n+j} = d_j$ and $\varphi_{n+j} = \varphi_j + \pi$ (modulo 2π). The side vectors of P are written as

$$s_j = \left\{ \begin{array}{ll} v_{k_{j+1}} - v_{k_j}, & c_j = 1, \\ v_{l_j} - v_{l_{j+1}}, & c_j = -1, \end{array} \right\} = c_j(z_{j+1} - z_j) =: c_j r_j \exp(i\rho_j) \quad \text{for } j = 1, \dots, n.$$

Hence, the construction of the generated zonogon Z implies that $s_j = c_j(z_{j+1} - z_j)$ for $j = 1, \dots, n$. We explicitly need to enforce that

$$0 = \sum_{j=1}^n s_j = \sum_{j=1}^n c_j(z_{j+1} - z_j), \quad (5)$$

so that the boundary curve of P is closed.

¹All indices k_j, l_j are understood as members of the residue system $\{1, \dots, n\}$ modulo n , which we shall silently assume for all upcoming index computations.

We are now ready to formulate the perimeter problem as the MINLP

$$\begin{aligned}
& \max \sum_{j=1}^n r_j \\
& \text{s.t. } 0 \leq r_j, \quad 0 \leq d_j \leq 1, \\
& \quad r_j \exp(i\rho_j) = d_{j+1} \exp(i\varphi_{j+1}) - d_j \exp(i\varphi_j), \quad j = 1, \dots, n, \\
& \quad \sum_{j=1}^n c_j r_j \exp(i\rho_j) = 0, \\
& \quad \varphi_1 \leq \varphi_2 \leq \dots \leq \varphi_{n+1} = \varphi_1 + \pi, \quad \rho_1 \leq \rho_2 \leq \dots \leq \rho_{n+1} = \rho_1 + \pi, \\
& \quad c_j \in \{\pm 1\}, \quad j = 1, \dots, n.
\end{aligned} \tag{6}$$

We solved all NLPs that result from MINLP (6) for each possible code c for $n = 4, 8, 16, 32$ numerically and found that $d_j = 1$ always held. Based on this numerical evidence, we now consider the case that P has a full set of n distinct diameters $v_k v_l$ with $|v_k - v_l| = 1$ (more are not possible, see [23]). This happens exactly if the zonogon Z is inscribed into the unit circle, i.e., all its vertices z_j , $j = 1, \dots, 2n$, lie on the unit circle. Then the problem allows for the following formulation as a MINLP

$$\begin{aligned}
& \max \sum_{j=1}^n 2 \sin \frac{\varphi_{j+1} - \varphi_j}{2} \\
& \text{s.t. } \sum_{j=1}^n c_j (\cos \varphi_{j+1} - \cos \varphi_j) = 0, \quad \sum_{j=1}^n c_j (\sin \varphi_{j+1} - \sin \varphi_j) = 0, \\
& \quad \varphi_1 \leq \varphi_2 \leq \dots \leq \varphi_{n+1} = \varphi_1 + \pi, \\
& \quad c_j \in \{\pm 1\}, \quad j = 1, \dots, n,
\end{aligned} \tag{7}$$

which comprises n continuous real variables $\varphi_1, \dots, \varphi_n$ and n “binary” variables c_1, \dots, c_n . The two equality constraints, which are the real and imaginary parts of (5), are nonlinear in φ . The continuous rotational symmetry of MINLP (7) can be eliminated by fixing one of the angles, e.g., $\varphi_1 = 0$.

The MINLP (7) is more general than the NLP proposed in [22], which is formulated for fixed compositions instead of codes that are still free for optimization. Furthermore, working with absolute angles instead of angle differences yields computationally more favorable sparsity structures, which we shall exploit in Sec. 4.

3 Code combinatorics

The codes c characterize the combinatorial structure of P and Z . Clearly, the perimeter problem allows for congruence transformations. So we only have to deal with the equivalence classes of codes with respect to the automorphism group of the cycle graph C_n , which is known to be isomorphic to the dihedral group D_n . To enumerate

the essentially distinct codes for the MINLPs (6) and (7) we propose two approaches, which are based on the zonogon and the polygon viewpoints.

3.1 Zonogon view

We consider again the zonogon Z with the code $c \in \{\pm 1\}^{2n}$ attached to its sides. Because $c_{n+j} = -c_j$, the equivalent codes can be considered as a self-dual two-colored (plus/minus) bracelet (turnover necklace) with $2n$ beads [24] with at most $n - 2$ consecutive beads of the same color. This restriction is caused by the fact that at most $n - 2$ sides of each P_l may be also sides of Z , because v_l has been moved to the origin, which is inside Z .

There is exactly one self-dual bracelet of length $2n$ with n consecutive beads:

$$(+ + \cdots + - - \cdots -).$$

Moreover, self-dual bracelets of length $2n$ with $n - 1$ consecutive beads do not exist, because they would need to have the form

$$\left(\underbrace{+ \cdots +}_{n-1 \text{ times}} - \underbrace{- \cdots -}_{n-1 \text{ times}} + \right),$$

which has n consecutive beads.

Hence, the number of essentially distinct codes is one less than the number of self-dual two-colored bracelets with $2n$ beads, which is known as sequence A007147 in the OEIS [25].

3.2 Vertex-oriented polygon view

Alternatively, we can enumerate codes by looking at the (undirected) diameter graph of the polygon P , which consists of the nodes $\{v_1, \dots, v_n\}$ and has edges connecting v_k and v_l if $|v_k - v_l| = 1$. Supposing a full set of n diameters, the edges of the diameter graph are in one-to-one correspondence with the code c through the sequences (l_j) and (k_j) because $z_j = v_{k_j} - v_{l_j}$. Coloring in red each vertex that is incident to only one edge (i.e., appears only once in each of the sequences (l_j) and (k_j)) and all other vertices white, we obtain a graph with two-colored nodes. After removal of all red nodes, the remaining part of the diameter graph must be an odd cycle (compare [23]). The zonogon construction informs us that there can be at most $n - 3$ red nodes and, hence, there must be at least three white nodes. In Fig. 4, for instance, the only red vertex would be v_3 because $l_6 = 3$ and $l_j \neq 3$ for all $j \neq 6$. Consequently, the number of distinct codes is equal to the number of bracelets with n beads colored white or red with an odd number of at least three white beads. This sequence is known as sequence A263768 in the OEIS [26].

As a consequence, we have just proved that

$$A263768(n) = A007147(n) - 1.$$

In Tab. 1 we see that although the number of distinct codes grows rapidly, we can completely enumerate all possible codes in a reasonable amount of time at least for $n \leq 32$ using fast algorithms [27].

3.3 Integer composition view

To encode diameter graphs, it is customary to use integer compositions of n , which are m -tuples of positive integers that sum up to n . It is not difficult to derive that there is a one-to-one correspondence to the codes $c \in \{\pm 1\}^{2n}$, by counting the number of consecutive negative entries or, equivalently, the number of consecutive positive entries.

As an example, the code $c = (+ - - + - + + - - + + - + - - +)$ of the optimal octagon leads to the composition $(2, 1, 2, 1, 2)$ by counting the consecutive minus signs. When counting consecutive signs, one has to consider the code as cyclic. Counting plus signs in the example leads to the composition $(1, 2, 2, 1, 2)$ or $(2, 1, 2, 2, 1)$, depending on whether the first plus is wrapped to the end or vice versa. All three compositions are equivalent. To recover a code from, e.g., the composition $(2, 1, 2, 2, 1)$, we first write down the consecutive groups of negative signs and then fill the blanks, starting left of the first minus group with plus signs going through the composition from its center entry $(2, 2, 1, 2, 1)$

$$(- - - - -) \rightsquigarrow (+ + - - + + - - + + - - + -),$$

which is equivalent to the original c under the action of the dihedral group D_{16} , in this particular case a shift by five to the right.

4 Two-phase algorithm using arbitrary precision arithmetic

We propose a two-phase algorithm that computes a code first (Phase I) and then computes a (local) solution of the fixed code NLP with an arbitrary precision Lagrange-Newton method (Phase II).

The approach is motivated by taking the regular $2n$ -gon for Z , i.e., choosing

$$\varphi_j^* = \frac{j\pi}{n} \quad \text{for } j = 1, \dots, 2n.$$

Inserting φ^* into MINLP (7), we immediately obtain that the objective coincides with Reinhardt's upper bound \bar{u}_n . The idea of Phase I is now to find a code $c^* \in \{\pm 1\}$ with minimal violation of the equality constraints, while in Phase II we fix $c = c^*$ and use variations of a local Lagrange-Newton method with initial guess (c^*, φ^*) (disregarding the angle inequalities).

4.1 Phase I: Subset-Sum Problem

Using φ^* , we obtain for $j = 1, \dots, 2n$ that

$$z_j^* = \exp(i\varphi_j^*) = \xi^j \quad \text{with } \xi = \exp(i\pi/n).$$

The complex-valued version (5) of the equality constraint function in MINLP (7) then becomes

$$r(c) := \sum_{j=1}^n c_j (z_{j+1}^* - z_j^*) = (\xi - 1) \sum_{j=1}^n c_j \xi^j.$$

Hence, minimizing the constraint violation means to pick n non-opposing $2n$ -th roots of unity such that their sum is as small as possible.

4.1.1 Case of odd divisors

We immediately observe that if n has an odd divisor $d \geq 3$, there are (possibly multiple) codes c^* for which $r(c^*)$ vanishes. In this case (c^*, φ^*) is already a global solution of MINLP (7) because it attains the upper bound \bar{u}_n . One simple construction for such a code is

$$c_j^* = (-1)^{\lceil \frac{jd}{n} \rceil} \quad \text{for } j = 1, \dots, 2n,$$

which satisfies

$$c_{n+j}^* = (-1)^{d + \lceil \frac{jd}{n} \rceil} = -c_j^*$$

and with the representation $j = p + q\frac{n}{d}$ for $p = 1, \dots, \frac{n}{d}$, $q = 0, \dots, d - 1$, also

$$\frac{r(c^*)}{\xi - 1} = \sum_{j=1}^n c_j^* \xi^j = \sum_{q=0}^{d-1} \sum_{p=1}^{n/d} (-1)^{q + \lceil \frac{pd}{n} \rceil} \xi^{p + \frac{qn}{d}} = \left(\sum_{q=0}^{d-1} (-\xi^{\frac{n}{d}})^q \right) \left(-\sum_{p=1}^{n/d} \xi^p \right) = 0,$$

because the first factor is the sum of all d -th roots of unity. If n is odd, an even simpler choice is $c_j^* = (-1)^j$.

4.1.2 Case of n a power of two

For $n = 2^s$, there is in general no code c^* with $r(c^*) = 0$ and the problem becomes an interesting variation on a challenging question about sums of roots of unity [28, 29].

Exploiting the dihedral symmetry of c^* inherent in MINLP (7), we can assume without loss of generality that $\arg r(c^*) \in [0, \frac{1}{2}\varphi_1^*]$ and minimize the real part of $r(c^*)$ (or do the same for $r(c^*)/(\xi - 1)$).

The computations become easier if we assume Mossinghoff's conjecture to be true: We can then resort to symmetric codes

$$c_{n-j+1} = -c_j \quad \text{for } j = 1, \dots, \frac{n}{2}. \tag{8}$$

Besides halving the degrees of freedom, this also leads to

$$\xi^{-1}r(c) = (1 - \xi^{-1}) \sum_{j=1}^n c_j \xi^j = \left(\xi^{\frac{1}{2}} - \xi^{-\frac{1}{2}} \right) \sum_{j=1}^n c_j \xi^{j-\frac{1}{2}} = 4i\Im \left(\xi^{\frac{1}{2}} \right) \sum_{j=1}^{n/2} c_j \Re \left(\xi^{j-\frac{1}{2}} \right)$$

being a purely imaginary quantity. Let us abbreviate

$$w_j := \Re \left(\xi^{j-\frac{1}{2}} \right) = \cos \left(\left(j - \frac{1}{2} \right) \frac{\pi}{n} \right).$$

We can then write the problem of minimizing the constraint violation as

$$\min w^T c \quad \text{s.t. } w^T c \geq 0, c \in \{\pm 1\}^{n/2}.$$

By substituting $c_j = 1 - 2x_j$, we arrive at the SSP with real coefficients

$$\max w^T x \quad \text{s.t. } w^T x \leq \frac{1}{2} \sum_{j=1}^{n/2} w_j, x \in \{0, 1\}^{n/2}. \quad (9)$$

SSPs are a special case of Knapsack Problems, which are known to be NP-hard. For an introduction, we refer the reader to [30]. Fully polynomial-time approximation schemes are of no help here, because the coefficients w are not rational, leading to extremely large constants that would lead to very extreme memory requirements.

4.2 Phase II: Code-restricted nonlinear problem

Now we fix the code c^* from Phase I and solve MINLP (7), where it is computationally advantageous to reorder the sums in the constraints and to fix φ_1 and φ_{n+1} to eliminate the continuous rotational symmetry. We obtain the NLP

$$\begin{aligned} \max \quad & \sum_{j=1}^n 2 \sin \frac{\varphi_{j+1} - \varphi_j}{2} =: -f(\varphi) \\ \text{s.t. } \quad & 0 = \sum_{j=2}^n (c_{j-1}^* - c_j^*) \cos \varphi_j - (c_1^* + c_n^*) =: g_1(\varphi), \\ & 0 = \sum_{j=2}^n (c_{j-1}^* - c_j^*) \sin \varphi_j =: g_2(\varphi), \\ & 0 = \varphi_1 \leq \varphi_2 \leq \dots \leq \varphi_{n+1} = \pi. \end{aligned} \quad (10)$$

Because the inequality constraints will not be active in the solutions we are interested in, we drop them in the remainder. We consider a numerical method of Lagrange-Newton-type for solving NLP (10).

The Lagrangian corresponding to NLP (10) without code symmetry exploitation reads

$$L(\varphi, y) = f(\varphi) + y_1 g_1(\varphi) + y_2 g_2(\varphi).$$

For $j = 2, \dots, n$, its first derivatives are

$$\frac{\partial L}{\partial \varphi_j}(\varphi, y) = \frac{1}{2} \left(\cos \frac{\varphi_{j+1} - \varphi_j}{2} - \cos \frac{\varphi_j - \varphi_{j-1}}{2} \right) + (c_{j-1}^* - c_j^*)(y_2 \cos \varphi_j - y_1 \sin \varphi_j).$$

The Hessian matrix H of L with respect to $\varphi_2, \dots, \varphi_n$ is tridiagonal and symmetric with diagonal entries

$$H_{jj}(\varphi, y) = \frac{1}{4} \left(\sin \frac{\varphi_{j+1} - \varphi_j}{2} + \sin \frac{\varphi_j - \varphi_{j-1}}{2} \right) + (c_j^* - c_{j-1}^*)(y_1 \cos \varphi_j - y_2 \sin \varphi_j)$$

for $j = 2, \dots, n$ and off-diagonal entries

$$H_{j,j+1}(\varphi, y) = H_{j+1,j}(\varphi, y) = -\frac{1}{4} \sin \frac{\varphi_j - \varphi_{j+1}}{2}$$

for $j = 2, \dots, n-1$. The entries of the constraint Jacobian C are for $j = 2, \dots, n$

$$C_{1j}(\varphi, y) = (c_j^* - c_{j-1}^*) \sin \varphi_j, \quad C_{2j}(\varphi, y) = (c_{j-1}^* - c_j^*) \cos \varphi_j.$$

Recalling that $\nabla_y L(\varphi, y) = g(\varphi)$, we can now perform a local Newton-type method on $w = (\varphi, y)$ according to

$$w^{k+1} = w^k - A_k \nabla L(w^k), \quad w^0 = \begin{pmatrix} \varphi^* \\ 0 \end{pmatrix} \quad \text{where } A_k^{-1} \approx K(w^k) := \begin{pmatrix} H(w^k) & C(w^k)^T \\ C(w^k) & 0 \end{pmatrix}.$$

It is important to use high-precision arithmetic to evaluate ∇L . Inaccuracies in A_k will reduce the convergence speed but will not change the fix points of the method, as long as A_k stays invertible. Possible numerical realizations of A_k are:

1. Direct sparse decomposition: Evaluate $H(w^k)$ and $C(w^k)$, round to double precision, and use an off-the-shelf direct sparse decomposition algorithm in double precision on the rounded block matrix $K(w^k)$. This leads to a linearly convergent algorithm, where typically ten to fifteen digits of accuracy are gained per iteration.
2. Schur complement: The symmetric tridiagonal $H(w^k)$ is easy to invert and the resulting Schur complement $-C(w^k)H^{-1}(w^k)C(w^k)^T$ is just a 2-by-2 matrix, which can also be easily inverted. All these operations can be performed in arbitrary precision arithmetic, which retains the locally quadratic convergence of the Newton method.
3. MINRES: Use the Krylov method MINRES [31] in high-precision arithmetic as a direct solver by performing $n+1$ MINRES iterations, which also retains locally quadratic convergence.
4. Simplified Newton variants: Take one of the first two approaches but always use the linearization in w^0 , i.e., always use A_0 instead of A_k . This yields considerable

speed-ups for each iteration. The rate of convergence, however, will be at most linear.

We establish next that $K(w)$ is indeed invertible in a neighborhood of $w^0 = w^*$.

Lemma 2. *If $0 < \varphi_2 < \dots < \varphi_n < \pi$, then $C(w)$ has rank two.*

Proof. Let us abbreviate the index set

$$J = \{j \in \{2, \dots, n\} \mid c_j^* \neq c_{j-1}^*\},$$

which has at least two elements. A direct computation reveals

$$\begin{aligned} & \det(C(w)C(w)^T) \\ &= \sum_{i,j=2}^n (c_i^* - c_{i-1}^*)^2 (c_j^* - c_{j-1}^*)^2 (\sin^2 \varphi_i \cos^2 \varphi_j - \sin \varphi_i \cos \varphi_i \sin \varphi_j \cos \varphi_j) \\ &= 16 \sum_{i,j \in J} (\sin^2 \varphi_i \cos^2 \varphi_j - \sin \varphi_i \cos \varphi_i \sin \varphi_j \cos \varphi_j) \\ &= 16 \sum_{i \in J} \sum_{\substack{j \in J \\ j > i}} (\sin^2 \varphi_i \cos^2 \varphi_j - 2 \sin \varphi_i \cos \varphi_i \sin \varphi_j \cos \varphi_j + \sin^2 \varphi_j \cos^2 \varphi_i) \\ &= 16 \sum_{i \in J} \sum_{\substack{j \in J \\ j > i}} \underbrace{(\sin \varphi_i \cos \varphi_j - \sin \varphi_j \cos \varphi_i)^2}_{=\sin(\varphi_i - \varphi_j) \neq 0} > 0. \end{aligned}$$

Hence, $C(w)C(w)^T$ has rank two, which is only possible if $C(w)$ has rank two. \square

Lemma 2 also shows that any non-degenerate configuration of angles satisfies the Linear Independence Constraint Qualification for NLP (10).

Lemma 3. *The Hessian matrix $H(w^*)$ is positive definite for $(\varphi^*, 0)$.*

Proof. By the definition of φ^* , we have for all $j = 2, \dots, n$ that

$$\sin \frac{\varphi_j^* - \varphi_{j-1}^*}{2} = \sin \frac{\pi}{2n}.$$

Hence,

$$H(w^*) = \frac{\sin \frac{\pi}{2n}}{4} \begin{pmatrix} 2 & -1 & & & \\ -1 & \ddots & \ddots & & \\ & \ddots & \ddots & -1 & \\ & & & -1 & 2 \end{pmatrix},$$

which has a complete set of eigenvectors $v^l \in \mathbb{R}^{n-1}$ of the form $v_j^l = \sin \frac{lj\pi}{n}$ because with the convention $v_0^l = v_n^l = 0$, a trigonometric identity yields for all $l = 1, \dots, n-1$ that

$$v_{j-1}^l + v_{j+1}^l = \sin \left(\frac{lj\pi}{n} - \frac{l\pi}{n} \right) + \sin \left(\frac{lj\pi}{n} + \frac{l\pi}{n} \right) = 2v_j^l \cos \frac{l\pi}{n}.$$

Hence, the eigenvalues of $H(w^*)$ are $\frac{1}{2}(1 - \cos \frac{l\pi}{n}) \sin \frac{\pi}{2n} > 0$ for $l = 1, \dots, n - 1$ and $H(w^*)$ is positive definite. \square

Lemma 4. *The block matrix $K(w)$ is invertible in a neighborhood of w^* .*

Proof. The constraint Jacobian $C(w^*)$ has full rank and the Hessian $H(w^*)$ is positive definite by Lemmas 2 and 3. Hence $K(w^*)$ is invertible. By continuity of K , it is invertible in a neighborhood of w^* . \square

Lemma 4 assures us that the simplified Newton variants have well-defined iterates, even though convergence is only guaranteed if a solution of NLP (10) is located sufficiently close to w^* .

The NLP (10) can be reduced further by exploiting structure in the code c^* , e.g., code symmetry as in Mossinghoff’s conjecture or by exploiting that pending diameters dissect the diameter graph cycle’s angles equally. We shall see in Sec. 5 that the real bottleneck of the two-phase approach is Phase I, so that further improvements for Phase II will not yield considerable computational improvements.

5 Computational experience

We want to provide information on the computational experiences we gained with the approaches put forward in Sec. 4.

5.1 Phase I

Up to $n = 32$, we enumerated all possible codes (without the additional symmetry of Mossinghoff’s conjecture) using the C program accompanying the paper [27].

We also experimented with minimizing the constraint violation in MINLP (7) for fixed $\varphi = \varphi^*$ using the angular constraints described at the beginning of Sec. 4.1.2 in Gurobi [32], which works well up to $n = 32$.

For $n \geq 64$, the default settings of Gurobi lead to acceptance of non-optimal iterates, which is due to double precision arithmetic incurring too large numerical errors. Experiments with tweaking the options `NumericFocus` to its maximum of 3 and enabling `Quad` for quadruple precision in the Simplex method were not enough to obtain reliable results. This applies also for the SSP problem (9) resulting from assuming Mossinghoff’s conjecture to be true.

Using the exact rational version of SCIP [33, 34] for extra precision to solve the SSP (9) was also unsuccessful. With default parameter settings, the solver ran into memory issues on a large machine with 500 GB of RAM. These memory issues can be mitigated by deactivating cut generation (option `separating/maxcuts=0`) and changing the node selection to depth-first-search (option `nodeselection/dfs/stdpriority=1000000`). The performance is, however, quite slow due to the usage of rational arithmetic and it appears that a large part of the branching tree must be visited.

Hence, we implemented two concise C programs, which can be obtained from the authors on reasonable request. The first uses GCC’s `libquadmath` quadruple floating point arithmetic, the second uses purely 128-bit integer arithmetic for rational numbers

in Tab. 3. We can see that for large n , the simplified Newton method performs highly efficiently.

The runtimes also show that the real bottleneck of the two-phase approach is Phase I. Additional structure exploitation, e.g., through reduced versions of NLP (10) is not necessary.

n	(Simplified*) Newton it.	Runtime [s]
4	10	0.02
8	10	0.03
16	9	0.16
32	17*	0.09
64	9*	0.02
128	8*	0.05

Table 5: Number of Phase II Newton iterations and corresponding runtime for different codes of length n from Phase I. For $n \geq 32$, a simplified Newton method was used, indicated by *.

6 The longest perimeter of a small octagon is algebraic

Phase I delivers a code c^* . As an alternative to Phase II, it is in some cases possible to derive the solution of the maximum perimeter problem for the fixed code c^* by analytical means.

6.1 Statements of the results

As mentioned in the introduction, the maximum area of a small hexagon received quite some attention. It occurs as *Graham's hexagon constant* in the fundamental encyclopedia [36, p. 526] and is available in Mathematica as `n=6; GraphData["BiggestLittlePolygon", n]`.² To some extent this popularity is based on its representation as an algebraic number.³ This suggests asking for similar results for the longest perimeter of a small octagon.

Here we demonstrate that the square of the longest perimeter of a small octagon is a root of an integer polynomial of degree 48. We obtained this polynomial by three independent approaches. The derivations are based on a formulation using cartesian coordinates or via a trigonometric formulation with half angle substitution. The most

²But be aware, the octagon data for $n = 8$ are quite inaccurate.

³It seems to be worthwhile to cite the comment by H. Hadwiger in [6]: Nun ist es H. Bieri (Bern) gelungen, das Problem für $n = 6$ im achsensymmetrischen Fall zu lösen. Hierbei ist einzuräumen, dass das extremale Polygon auch im allgemeinen Fall achsiale Symmetrie aufweisen dürfte, so dass die gefundene Lösung vermutlich allgemeine Gültigkeit hat. Die von Bieri erzielte Lösung ist indessen nicht einfach angebar, und die Form, in der die eindeutige Kennzeichnung des extremalen Polygons und des maximalen Flächeninhaltes erfolgen muss, regt an, sich über den Begriff Lösung eines elementargeometrischen Problems einige nützliche Gedanken zu machen.

efficient approach uses Lagrange multipliers. The application of this idea to Graham's hexagon is somewhat hidden as an example in [9, p. 46]. Therefore, we begin with revisiting the small hexagon and the small octagon of largest area. We also consider the case of equilateral small octagons and derive a polynomial of degree 6 for the corresponding longest perimeter. This polynomial has already been mentioned without proof in [37].

Our derivations rely on algorithms dealing with ideals of multivariate polynomials with integer coefficients. We carried out all computations using implementations of such algorithms in SageMath [38] as well as in Mathematica [39]. We only provide brief descriptions of our approach, which are not to be considered as complete proofs.

Proposition 1. *The square of the maximum perimeter $p_8 \approx 3.12114713405983$ of a small octagon is a root of an integer polynomial P_8 of degree 48, see [Appendix A](#). The maximum perimeter $e_8 = 8s_8 \approx 3.095609317476962$ of an equilateral small octagon belongs to the side length s_8 , which is a root of the integer polynomial*

$$E_8(t) = 2t^6 - 18t^5 + 57t^4 - 78t^3 + 46t^2 - 12t + 1$$

of degree 6.

We include a formulation of the results concerning the maximum area, since we are going to present alternative derivations.

Proposition 2 ([3, 7]). *The maximum area $a_6 \approx 0.6749814429301$ of a small hexagon is a root of the integer polynomial*

$$A_6(t) = 4096t^{10} + 8192t^9 - 3008t^8 - 30848t^7 + 21056t^6 + 146496t^5 \\ - 221360t^4 + 1232t^3 + 144464t^2 - 78488t + 11993$$

of degree 10. The maximum area $a_8 \approx 0.726868482751$ of a small octagon is a root of an integer polynomial A_8 of degree 42, see [7].

6.2 The largest area small hexagon and octagon

6.2.1 Lagrange multipliers for the nonsymmetric hexagon

The enumeration of the vertices is illustrated in [Figure 5](#).

The vertices of the hexagon are parametrized by

$$v_1 = (x_1, y_1), \quad v_2 = (x_2, y_2), \quad v_3 = (0, 1), \\ v_4 = (x_4, y_4), \quad v_5 = (-x_1, y_1), \quad v_6 = (0, 0).$$

The symmetry of v_1 and v_5 incorporates the fact that the pending diameter chord v_3v_6 , which we fix, needs to be perpendicular to v_1v_5 for maximum area. We also emphasize that we do not require full symmetry through the line v_6v_3 . In fact, our derivation shows this symmetry property of the extremal hexagon to hold. Expressing the area t in terms of the variables gives the problem

$$\max_{x_1, y_1, x_2, y_2, x_4, y_4} t = (x_2 + x_4(y_1 - 1) - x_2y_1 + x_1(y_2 + y_4))/2 \quad \text{subject to}$$

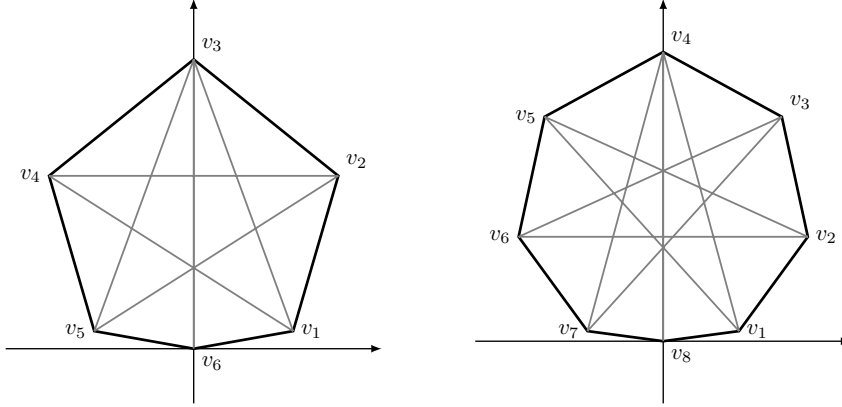


Fig. 5: The small hexagon and the small octagon of largest area. Both are symmetric through the (vertical) pending diameter chord.

$$|v_1 - v_3|^2 = |v_1 - v_4|^2 = |v_2 - v_4|^2 = |v_2 - v_5|^2 = 1.$$

We obtain the Lagrange function

$$L = t + \lambda_1(|v_1 - v_3|^2 - 1) + \lambda_2(|v_1 - v_4|^2 - 1) \\ + \lambda_3(|v_2 - v_4|^2 - 1) + \lambda_4(|v_2 - v_5|^2 - 1)$$

and the system

$$\frac{\partial L}{\partial x_1} = 0, \dots, \frac{\partial L}{\partial \lambda_4} = 0. \quad (11)$$

This resulting Lagrange system is a system of polynomial equations in the variables $t, x_1, y_1, x_2, y_2, x_4, y_4$ and four multipliers. The basic polynomial in the single variable t , that means in the area, is computed by `GroebnerBasis` as

$$B(t) = A_6(-t)A_6(t)Q(t), \quad (12)$$

where Q is of degree 18 in t^2 .

The symmetry assumption would reduce the problem by explicitly setting $x_2 = -x_4 = \frac{1}{2}$, $y_4 = y_2$, and $\lambda_3 = \lambda_4 = 0$, and would give the polynomial A_6 without any factorization.

6.2.2 Lagrange multipliers for the symmetric octagon

Here we completely exploit the known symmetry and incorporate it in the problem formulation. The vertices of the octagon are

$$v_1 = (x_1, y_1), \quad v_2 = \left(\frac{1}{2}, y_2\right), \quad v_3 = (x_3, y_3), \quad v_4 = (0, 1),$$

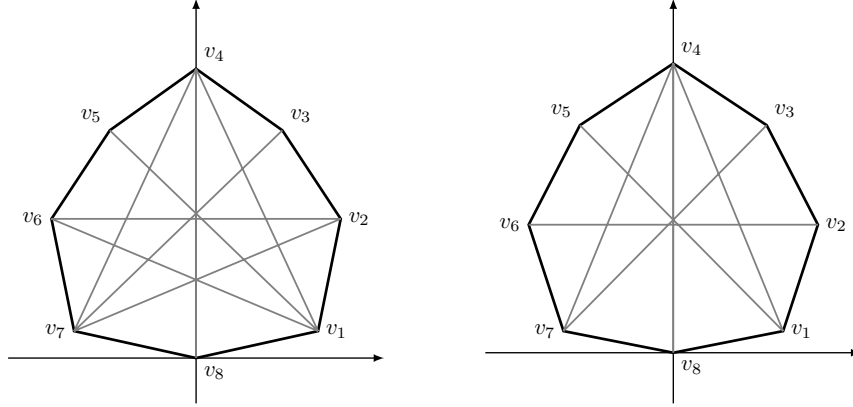


Fig. 6: The small octagon and the equilateral small octagon of longest perimeter. Both are symmetric, the equilateral solution has only six diameter chords.

$$v_5 = (-x_3, y_3), \quad v_6 = \left(-\frac{1}{2}, y_3\right), \quad v_7 = (-x_1, y_1), \quad v_8 = (0, 0),$$

its area is then given by

$$t = x_3 - x_3 y_2 + (-y_1 + 2x_1 y_2 + y_3)/2$$

and there remain the constraints $|v_1 - v_4|^2 = |v_1 - v_5|^2 = |v_2 - v_5|^2 = |v_2 - v_6|^2 = 1$. The corresponding Lagrange system is then reduced to the polynomial, which was already derived in [7].

6.3 The longest perimeter small octagon

As evident from [14] and from our computations, the extremal octagon P has eight diagonals of unit length. This diameter graph consists of a cycle of five edges and three pending edges. The octagon P is symmetric through one of the pending edges. For an illustration and our notation see Figure 6.

6.3.1 Half-angle substitution

We consider the angles $\alpha = \frac{1}{2}\angle v_4 v_1 v_6$ and $\beta = \frac{1}{4}\angle v_1 v_4 v_7$, which implies $\frac{1}{2}\angle v_6 v_2 v_7 = \pi/4 - \alpha - \beta$. Now, the extremal problem is formulated as

$$\begin{aligned} \max_{\alpha, \beta} \quad & 8 \sin \frac{\alpha}{2} + 4 \sin \beta + 4 \sin(\pi/4 - \alpha - \beta) \\ \text{s.t.} \quad & 2 \sin(2\beta) + 2(1 - \cos(\pi/2 - 2\alpha - 2\beta)) = 1. \end{aligned}$$

Note that the constraint is related to the length $|v_6 - v_2| = 1$. Using the substitutions $x = \tan(\alpha/4)$, $y = \tan(\beta/2)$, this problem becomes a rational system. The Mathematica functions `Resultant` and `Discriminant` deliver a polynomial of degree 48 in t in integers extended by $\sqrt{2}$, which is equivalent to the one given in Appendix A.

6.3.2 Lagrange multipliers

Respecting the symmetry through the pending diameter chord v_8v_4 , the vertices of P are shifted vertically downwards and parameterized by

$$\begin{aligned} v_1 &= (x, 0), & v_2 &= \left(\frac{1}{2}, v_2\right), & v_4 &= (0, 1 + y_8), \\ v_6 &= \left(-\frac{1}{2}, y_2\right), & v_7 &= (-x, 0), & v_8 &= (0, y_8). \end{aligned}$$

The vertex v_3 has to be the midpoint of the arc v_2v_4 of the circle around v_7 of unit radius. Introducing the slack variables $h_1 = |v_1 - v_8|$, $h_2 = |v_2 - v_1|$, $h_3 = |v_3 - v_2| = |v_4 - v_3|$, this implies the relation $|v_4 - v_2|^2 + h_3^4 - 4h_3^2 = 0$. Hence, the extremal problem may be written as

$$\begin{aligned} \max_{x, y, v} & 2(h_1 + h_2 + 2h_3) \\ \text{s.t.} & |v_1 - v_4|^2 = |v_2 - v_7|^2 = 1, \quad |v_1 - v_8|^2 = h_1^2, \quad |v_2 - v_1|^2 = h_2^2, \\ & |v_4 - v_2|^2 + h_3^4 - 4h_3^2 = 0. \end{aligned}$$

The Lagrange system is a polynomial system in the variables $p, x, y_2, y_8, h_1, h_2, h_3$ and five multipliers. The function `GroebnerBasis` in Mathematica easily comes up with the announced polynomial for the perimeter t .

As described above, we elaborated on a purely numerical two-phase approach for computing the maximum perimeters of small polygons. As a sanity check, the results for the root p_8 of the integer polynomial are identical with the ones reported in Tab. 2.

7 Conclusions

We derived two new MINLP formulations for computing lower bounds for Reinhardt's perimeter problem, which is still an open problem after more than 100 years. We argue that the derived lower bounds are strict if it is true that optimal polygons have a complete set of diameters. We propose a two-phase approach that consists of a (generalized) SSP to compute the best code, for which the regular n -gon, which realizes Reinhardt's upper bound, is almost feasible. Then we refine the regular n -gon in the second phase to a feasible polygon with large perimeter using an arbitrary precision Lagrange-Newton-type method. We share ample computational experience and provide high-accuracy solution candidates up to $n = 64$ and a probably suboptimal candidate for $n = 128$ with large perimeter. We further show that the perimeter of the octagon with largest perimeter is an algebraic number and provide the corresponding integer polynomials of degree 48.

Declarations

The authors declare that they have no known competing financial or non-financial interests that could have appeared to influence the work in this paper.

Appendix A The polynomial of the longest perimeter small octagon

Here we provide the integer coefficients of the polynomial derived in Sec. 6, which can also be used to compute the longest perimeter as a root of this polynomial to arbitrary precision.

$$\begin{aligned}
 q_8(t) = & t^{48} - 2688 t^{47} + 3446272 t^{46} - 2807592960 t^{45} + 1633674266624 t^{44} \\
 & - 723588467449856 t^{43} + 2538898109167370, 24 t^{42} \\
 & - 72517854035614629888 t^{41} + 17195167136435692371968 t^{40} \\
 & - 3434820210452081718329344 t^{39} + 584574334125421235902873600 t^{38} \\
 & - 85517739615251895256392663040 t^{37} + 10829446302748698450583070179328 t^{36} \\
 & - 1193816644613689654665612818907136 t^{35} + 115086843866723348026033261837811712 t^{34} \\
 & - 9738082617441544437635181820812197888 t^{33} \\
 & + 725423774155626603530948947333269684224 t^{32} \\
 & - 47694399655201711781649368889348291821568 t^{31} \\
 & + 2773474766447168322184997293630827538677760 t^{30} \\
 & - 142915937585753382520287017253466824236859392 t^{29} \\
 & + 6537352911881897599073318260145551517258088448 t^{28} \\
 & - 265914881136849371015171799699357177396926087168 t^{27} \\
 & + 9635371582576344208603139477144787322898164482048 t^{26} \\
 & - 311558095037500866248196651997764943419255015079936 t^{25} \\
 & + 9003894302377052774819990635603424836273155562536960 t^{24} \\
 & - 232798593505589953724659815997148521459619251942850560 t^{23} \\
 & + 5384698849214794614511096063213254330174249732122083328 t^{22} \\
 & - 111229883050697265095697776791662655429798099484617474048 t^{21} \\
 & + 2043943451881331447819048584603121094991258075349364244480 t^{20} \\
 & - 33204170232890601212009526399439211418502869355381160673280 t^{19} \\
 & + 472940328670015419031704476959013624500278043685261018136576 t^{18} \\
 & - 5852634224113275457409744736043691759211050964981756612050944 t^{17} \\
 & + 62479370348335228971031421065092236129622542636279079783890944 t^{16} \\
 & - 576375293461315675942032249195563488574543633050881901599916032 t^{15} \\
 & + 4710488377079952771836133728493511544552402556895090911062523904 t^{14} \\
 & - 36368623222587641069111818667387388732204823767000547849301655552 t^{13} \\
 & + 286657343740444279969083463862811708030275860108457118864141975552 t^{12} \\
 & - 2300409752638978585592882084275762121478341006958876960731097464832 t^{11} \\
 & + 17022846567049524499840649827179007136206891115523021868856676188160 t^{10} \\
 & - 105271885062338881752377059792380965744985216725352909959696593453056 t^9 \\
 & + 519661898036620827612298078628038297122538078160606821748651700781056 t^8
 \end{aligned}$$

$$\begin{aligned}
& - 205821861869524265019727161560558949852146590089048796155456777222656 t^7 \\
& + 6790786688361483921080280822642541944806188768497117715297100944637952 t^6 \\
& - 18953181950142721458054232615448184781228851292920395499757235462995968 t^5 \\
& + 42033580403345828191224614534012438972659544181809655477758966164881408 t^4 \\
& - 66202009827628255733947076652696118184733299289788671027802646213820416 t^3 \\
& + 66152337375333098717233438245411622983399457619149468736826967974739968 t^2 \\
& - 36757562971957762256433166768884793509267603912864060192884364027101184 t \\
& + 8563803984117479982232573393172818348276610047246959316838387256655872
\end{aligned}$$

References

- [1] Reinhardt, K.: Extremale Polygone gegebenen Durchmessers. Jahresbericht der Deutschen Mathematiker-Vereinigung **31**, 251–270 (1922)
- [2] Dolan, E.D., Moré, J.J., Munson, T.S.: Benchmarking optimization software with COPS 3.0. Technical report, Argonne National Lab., Argonne, IL (United States) (2004)
- [3] Graham, R.L.: The largest small hexagon. J. Combin. Theory Ser. A **18**, 165–170 (1975)
- [4] Audet, C., Hansen, P., Messine, F., Xiong, J.: The largest small octagon. J. Combin. Theory Ser. A **98**(1), 46–59 (2002)
- [5] Foster, J., Szabo, T.: Diameter graphs of polygons and the proof of a conjecture of Graham. J. Combin. Theory Ser. A **114**(8), 1515–1525 (2007)
- [6] Bieri, H.: Ungelöste Probleme: Zweiter Nachtrag zu Nr. 12. Elem. Math **16**, 105–106 (1961)
- [7] Audet, C., Hansen, P., Svrtan, D.: Using symbolic calculations to determine largest small polygons. J Global Optim **81**(1), 261–268 (2020)
- [8] Griffiths, D., Culpin, D.: Pi-optimal polygons. Math. Gaz. **59**(409), 165–175 (1975)
- [9] Trott: The Mathematica GuideBook for Symbolics. Springer, New York, NY (2006). <http://link.springer.com/10.1007/0-387-28815-5>, Accessed 2023-10-04
- [10] Hare, K.G., Mossinghoff, M.J.: Sporadic Reinhardt polygons **49**(3), 540–557 (2013)
- [11] Hare, K.G., Mossinghoff, M.J.: Most Reinhardt polygons are sporadic. Geom. Dedicata **198**, 1–18 (2019)
- [12] Taylor, S.J.: Some simple geometrical extremal problems **37**, 188–198 (1953)

- [13] Tamvakis, N.K.: On the perimeter and the area of the convex polygon of a given diameter. *Bull. Greek Math. Soc* **28**, 115–132 (1987)
- [14] Audet, C., Hansen, P., Messine, F.: The small octagon with longest perimeter. *J. Combin. Theory Ser. A* **114**(1), 135–150 (2007)
- [15] Mossinghoff, M.J.: A \$1 problem. *Amer. Math. Monthly* **113**(5), 385–402 (2006)
- [16] Mossinghoff, M.J.: Isodiametric problems for polygons. *Discrete Comput. Geom.* **36**(2), 363–379 (2006)
- [17] Gashkov, S.: Inequalities for the area and perimeter of a convex polygon (in Russian). *Kvant* **10**, 15–19 (1985)
- [18] Datta, B.: A discrete isoperimetric problem. *Geom. Dedicata* **64**(1), 55–68 (1997)
- [19] Fejes Tóth, G.: Finite variations on the isoperimetric problem. In: Fejes Tóth, L., Fejes Tóth, G., Kuperberg, W. (eds.) *Lagerungen: Arrangements in the Plane, on the Sphere, and in Space*. Grundlehren der mathematischen Wissenschaften, pp. 243–247. Springer, Cham (2023)
- [20] Bingane, C., Audet, C.: Tight bounds on the maximal perimeter of convex equilateral small polygons. *Arch. Math. (Basel)* **119**(3), 325–336 (2022)
- [21] Bingane, C.: Tight bounds on the maximal perimeter and the maximal width of convex small polygons. *J. Global Optim.* **84**(4), 1033–1051 (2022)
- [22] Bingane, C.: Maximal perimeter and maximal width of a convex small polygon. *arXiv* (2023). <https://doi.org/10.48550/arXiv.2106.11831>.
- [23] Erdős, P.: On sets of distances of n points. *Amer. Math. Monthly* **53**, 248–250 (1946)
- [24] Palmer, E.M., Robinson, R.W.: Enumeration of self-dual configurations. *Pacific J. Math.* **110**(1), 203–221 (1984)
- [25] The On-Line Encyclopedia of Integer Sequences (2023). <https://oeis.org/A007147> Accessed 2024-03-13
- [26] The On-Line Encyclopedia of Integer Sequences (2023). <https://oeis.org/A263768> Accessed 2024-03-13
- [27] Sawada, J.: Generating bracelets in constant amortized time. *SIAM Journal on Computing* **31**(1), 259–268 (2001)
- [28] Myerson, G.: Unsolved Problems: How Small Can a Sum of Roots of Unity Be? *Amer. Math. Monthly* **93**(6), 457–459 (1986)

- [29] Christie, L., Dykema, K.J., Klep, I.: Classifying minimal vanishing sums of roots of unity. arXiv (2020)
- [30] Kellerer, H., Pferschy, U., Pisinger, D.: Knapsack Problems, p. 546. Springer, Berlin (2004)
- [31] Paige, C.C., Saunders, M.A.: Solutions of sparse indefinite systems of linear equations. *SIAM J. Numer. Anal.* **12**(4), 617–629 (1975)
- [32] Gurobi Optimization, LLC: Gurobi Optimizer Reference Manual (2023). <https://www.gurobi.com>. Accessed 2024-03-13
- [33] Bestuzheva, K., Besançon, M., Chen, W.-K., Chmiela, A., Donkiewicz, T., Doornmalen, J., Eifler, L., Gaul, O., Gamrath, G., Gleixner, A., Gottwald, L., Graczyk, C., Halbig, K., Hoen, A., Hojny, C., Hulst, R., Koch, T., Lübbecke, M., Maher, S.J., Matter, F., Mühmer, E., Müller, B., Pfetsch, M.E., Rehfeldt, D., Schlein, S., Schlösser, F., Serrano, F., Shinano, Y., Sofranac, B., Turner, M., Vigerske, S., Wegscheider, F., Wellner, P., Weninger, D., Witzig, J.: Enabling research through the SCIP Optimization Suite 8.0. *ACM Trans. Math. Softw.* **49**(2) (2023)
- [34] Cook, W., Koch, T., Steffy, D.E., Wolter, K.: A hybrid branch-and-bound approach for exact rational mixed-integer programming. *Math. Program. Comput.* **5**(3), 305–344 (2013)
- [35] Davis, T.A.: Algorithm 832: UMFPACK V4.3—an unsymmetric-pattern multifrontal method. *ACM Trans. Math. Software* **30**(2), 196–199 (2004) <https://doi.org/10.1145/992200.992206>
- [36] Finch, S.R.: *Mathematical Constants. Encyclopedia of Mathematics and Its Applications*, vol. v. 94, 169. Cambridge University Press, New York (2003)
- [37] Bingane, C., Audet, C.: Tight bounds on the maximal perimeter of convex equilateral small polygons. *Arch. Math.* **119**(3), 325–336 (2022)
- [38] Stein, W.A., et al.: Sage Mathematics Software (Version 10.2). The Sage Development Team, (2024). The Sage Development Team. <http://www.sagemath.org>. Accessed 2024-03-13
- [39] Wolfram Research, Inc.: Mathematica, Version 14.0. Champaign, IL, 2024. <https://www.wolfram.com/mathematica>. Accessed 2024-03-13